Rapid Communications

Exotic superconductivity in noncentrosymmetric and magnetic $CeNiC_2$ revealed under high pressure

Susumu Katano,[1] Masayuki Ito,[1] Kohei Shibata,[1] Jun Gouchi,[2] Yoshiya Uwatoko,[2] Kazuyuki Matsubayashi,[3] Hideto Soeda,[4] and Hiroki Takahashi[4]

[1]*Department of Physics, Graduate School of Science and Engineering, Saitama University, Sakura-ku, Saitama, Saitama 338-8570, Japan*
[2]*The Institute of Solid State Physics, The University of Tokyo, Kashiwano-ha 5-1-5, Kashiwa, Chiba 277-8581, Japan*
[3]*Department of Engineering Science, The University of Electro-Communications, Chofu, Tokyo 182-8585, Japan*
[4]*Department of Physics, College of Humanities and Sciences, Nihon University, Sakurajosui 3-25-40, Setagaya-ku, Tokyo 156-8550, Japan*

(Received 14 September 2018; revised manuscript received 18 February 2019; published 7 March 2019; corrected 17 December 2019)

We have found that magnetically ordered noncentrosymmetric $CeNiC_2$ exhibits superconductivity under very high pressures of near 11 GPa. The transition temperature T_c is 3.5 K, the *highest* in all Ce heavy-fermion superconductors, implying quite strong electron pairings with a high-energy scale. Several physical quantities show diverging features of a quantum phase transition, however, its criticality appears in a rather narrow range of pressure. The upper critical field $\mu_0 H_{c2}(T = 0)$ is estimated to be 18 T, much higher than the Pauli paramagnetic limiting field of 6.5 T, indicating spin-triplet electron pairings correlated with its noncentrosymmetric structure.

DOI: 10.1103/PhysRevB.99.100501

Superconductivity (SC), an extraordinary state, was first explained by Bardeen, Cooper, and Schrieffer (BCS) with phonon-mediated electron pairs of spins with the opposite direction [1]. This spin-singlet *s*-wave state is frequently called *conventional*. The discoveries of high-T_c cuprates and heavy-fermion superconductors in these thirty years, however, have significantly deepened our understanding of pairing mechanisms and symmetries. The origin of the pairing in these *unconventional* systems is believed to be spin fluctuations (SFs). There, electrons are paired in a spin-singlet *d*-wave state, or in a spin-triplet *p*- or *f*-wave one.

Since the proposition by Anderson [2], it has been thought that spin-triplet states would not be compatible with noncentrosymmetric (NCS) structures. However, the advent of SC in NCS $CePt_3Si$ has changed the situation [3]. Recent theories show that NCS leads to the indistinguishability of spin-singlet and spin-triplet electron pairings, and thus to the coexistence of them *in general*. The lack of inversion symmetry causes antisymmetric spin-orbit coupling (ASOC), and triplet pairings are favorably formed under certain conditions [4]. The triplet states of strongly correlated NCS systems are characterized by a high upper critical field $\mu_0 H_{c2}$.

The ternary lanthanide nickel carbides $RNiC_2$ (*R*: rare-earth elements) crystallize in orthorhombic $CeNiC_2$-type NCS structures (space group *Amm*2); the lattice lacks inversion symmetry along the *c* axis. Refer to Fig. 1 in Ref. [5]. Its Ni and dimerized C atoms are located in the $a/2$ plane. Each of them forms a triangular lattice and together they form a hexagonal-like structure. These NiC_2 and *R* layers are stacked alternatively.

The system with $R =$ La is a Pauli paramagnet and exhibits SC below about 3 K; owing to its NCS, unusual electron pairings are expected. Some experiments suggest a spin-triplet state with nodal energy gaps, but others indicate a conventional spin-singlet BCS type with full gaps. To reconcile them, a novel nonunitary triplet state with even parity gap symmetry was recently proposed [6]. The situation is thus still puzzling [6,7].

$CeNiC_2$ indicates a marked contrast to $LaNiC_2$. The system does not condense into SC. Ce atoms possess localized magnetic moments, and form unique successive magnetic orderings (MOs): from a paramagnetic (P) to an incommensurate antiferromagnetic (AFIC) at 20 K, then to a commensurate antiferromagnetic (AFC) below about 10 K, and further to a ferromagnetic or ferrimagnetic (F) state at 2 K [8,9]. Noted that those antiferromagnetic states seem to contain ferromagnetic components also [9]. In AFC, neutron diffraction indicated that magnetic moments, estimated to be $0.25\mu_B$, order along the *b* axis [8]. A recent study on the electronic and magnetic properties of (La and Ce)NiC_2 clarified the differences between them; strongly correlated heavy-fermion natures are considerably enhanced in $CeNiC_2$ owing to the $4f$-electron characters of Ce [5].

In this Rapid Communication, we perform resistivity and magnetic susceptibility measurements under pressures up to 15 GPa. Here, we observe conspicuous changes of MO with increasing pressure and discover a transition to SC with a T_c as high as 3.5 K. The quantum critical (QC) behavior occurs rather dramatically. Further, we found that $\mu_0 H_{c2}$ is quite high, over 18 T at $T = 0$. The pairing mechanism and symmetry of this SC are discussed.

A polycrystalline sample of $CeNiC_2$ was synthesized with Ce (3N), Ni (4N8), and C (5N5) in an argon-arc furnace. Details on the sample preparation are shown in Ref. [5]. An x-ray diffraction was employed to check sample qualities. The diffraction pattern at ambient pressure showed that the specimen has orthorhombic *Amm*2 without any significant impurity phases. The lattice constants determined are that $a = 3.882(1)$, $b = 4.556(1)$, and $c = 6.172(2)$ Å. The x-ray

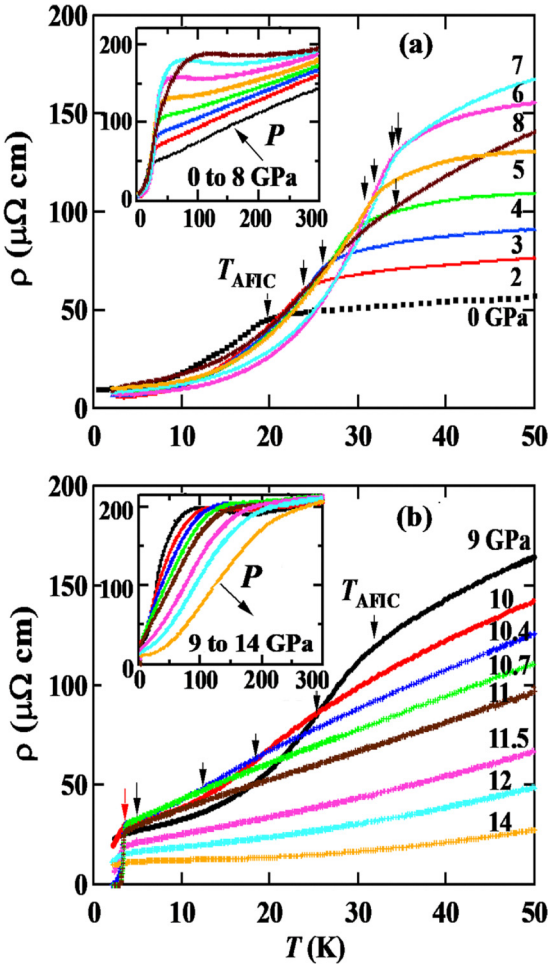

FIG. 1. Electrical resistivity of $CeNiC_2$ under high pressures below 50 K. (a) The data from 0 to 8 GPa. (b) Those from 9 to 14 GPa. The black arrows indicate the transition temperatures T_{AFIC}. SC is observed at 3.5 K under pressures around 11 GPa, shown with the (red) arrow. The insets display the resistivity up to 300 K.

diffraction examined up to 16 GPa shows that this *Amm*2 NCS structure is kept under high pressure. The unit-cell volume is decreased linearly by 7.6(4)% for 16 GPa, i.e., the compressibility is $0.47(3) \times 10^{-11}$ m^2/N [10].

The data under high pressures up to 15 GPa were collected with a cubic-anvil-type high-pressure apparatus between 2 K and room temperature. A teflon capsule (with a diameter of 1.5 mm at ambient pressure) with a transmitting medium of glycerol retains pressure hydrostatically. This teflon capsule was placed in a cubic-type integrated-fin gasket ($5 \times 5 \times 5$ mm^3) made of MgO [11]. The electric resistivity was measured by the conventional four-probe method, and the susceptibility by the ac induction technique with a frequency of 317 Hz. The resistivity in the magnetic fields was measured using a superconducting magnet up to 5 T. The pressure was determined by the superconducting transition of Pb.

The temperature dependences of the electrical resistivity ρ are shown in Fig. 1(a) for the data from 0 to 8 GPa, and Fig. 1(b) for those from 9 to 14 GPa. At ambient pressure ρ decreases with decreasing temperature and exhibits a steep fall below 20 K, where $d\rho/dT$ shows an apparent anomaly;

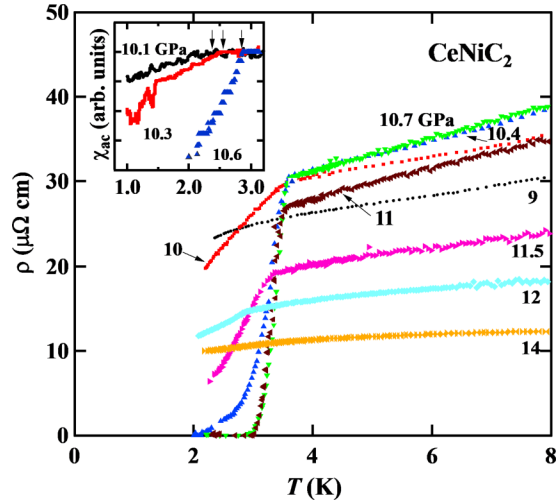

FIG. 2. Electrical resistivity near 11 GPa and below 8 K. The inset shows the ac magnetic susceptibility, indicating diamagnetic signals.

they indicate the transition temperature to AFIC, T_{AFIC}, shown with a black arrow in Fig. 1(a). With increasing pressure T_{AFIC} substantially increases from 20 K at a rate of 2.4 K/GPa, reaching a maximum at about 35 K under 6 and 7 GPa.

For AFC and F, anomalies are *not* obvious in ρ itself and also in $d\rho/dT$; thus those transitions were determined with specific heat before [5]. Here, we decide them by dc magnetization using a superconducting quantum interference device (SQUID) magnetometer; however, because of a limit of the pressure apparatus used (a piston-cylinder-type cell made of Cu-Be alloys), those temperatures have been determined only up to 2 GPa. The results indicate that the transitions to AFC and F do not change largely. The determination of their transition temperatures is important, but precise specific heat measurements under the 10-GPa class were difficult.

Above around 6 GPa the resistivity above 60 K shows sign of a decrease, indicating Kondo behavior as $-\ln T$. The resistivity at the higher temperatures increases with the phonon resistivity; see the inset of Fig. 1(a). At 8 GPa, the raw resistivity shows no clear anomaly with T_{AFIC}, implying that the MO starts to break down. There, an anomaly in $d\rho/dT$ is apparent, which determines the AFIC transition. This transition rapidly decreases with pressure, as shown by the black arrows in Fig. 1(b).

At about 10 GPa, with a collapse of MO, the resistivity falls suddenly below about 3 K (an emergence of SC). Figure 2 shows the data around 11 GPa below 8 K. The SC was observed under pressures of 10.7 and 11 GPa at 3.5 K. These transitions are fairly sharp with a width of less than 0.4 K. Taking into account that the sample examined is a polycrystal consisting of many grains and there may exist a nonuniformity of pressure surrounding the sample, the *intrinsic* transition is expected to be sharp as well; thus, T_c can be considered to be 3.5 K. The ac magnetic susceptibility under these pressures is indicated in the inset of Fig. 2, showing the diamagnetism associated with SC. Since the magnitude of the signal around 11 GPa is as large as that from Pb, the pressure gauge, the SC is of a bulk origin. The T_c observed is quite high compared

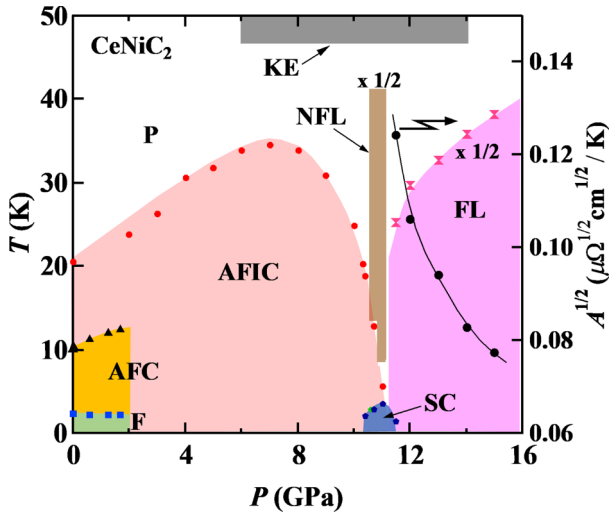

FIG. 3. P-T phase diagram. Magnetic states: P, AFIC, AFC, and F. The transition temperatures for AFC and F could be obtained only up to 2 GPa. See text. Pressure reveals SC, NFL, FL, and KE. A is the coefficient of the T^2 dependence of the resistivity. The temperatures for NFL, FL, and KE are multiplied by a factor of 1/2.

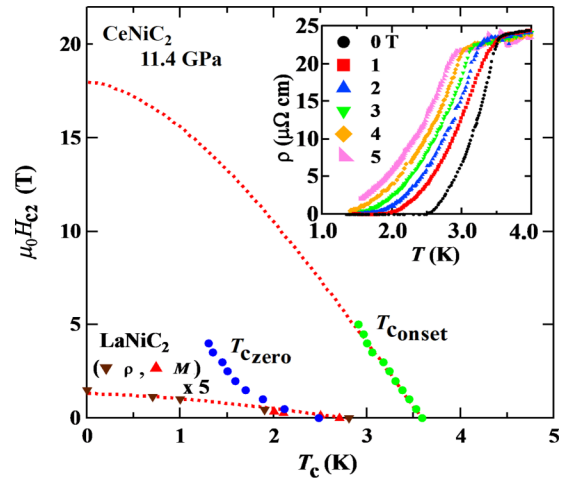

FIG. 4. $\mu_0 H_{c2}$ vs T_c determined from the field dependence of the resistivity under 11.4 GPa shown in the inset. $\mu_0 H_{c2}$ at $T = 0$ is estimated to be 18 T. That for $LaNiC_2$, at ambient pressure, is about 0.3 T; the data are multiplied by a factor of 5. The dotted lines show the fits to the WHH theory.

with that of other NCS Ce-based superconductors whose T_c's are of the order of 1 K [3,12–14], and furthermore, with that of all Ce heavy-fermion superconductors whose highest T_c is 2.6 K of $CeCoIn_5$ [15].

Under 10.7 and 11 GPa only, the resistivity above T_c increases in proportion to T up to about 80 K, as shown in Fig. 1(b) and its inset. This shows a non-Fermi-liquid (NFL) behavior. Such a linear-T dependence was predicted for two-dimensional (2D) AF SF [16]. These results imply that the SC found is not a conventional BCS type mediated with phonons but is an unconventional one with some magnetic origin. The high T_c observed may be correlated *first* with strong SF, accompanied by the collapse of MO with high transition temperatures.

Above 12 GPa the SC disappears and the low-temperature resistivity follows AT^2; see the resistivity in Fig. 1(b) which displays an upward curvature. This shows a change to a Fermi-liquid (FL) character. The coefficient A represents the strength of the interaction between conduction electrons. A and the residual resistivity ρ_0 obtained from the data exhibit a peak at around 11 GPa and decrease rapidly under higher pressures. These results indicate a QC behavior, and changes from an enhanced strongly correlated metal to a normal one.

These results are summarized in the P-T phase diagram of Fig. 3. As described above, the phase diagram shows the enhancement and collapse of MO, the emergence of SC and NFL, and then the change to FL, with pressure. The regions for NFL and FL were determined from the temperatures where the resistivity depends on T and T^2, respectively. The phase diagram acquired is similar to that of heavy-fermion superconductors with MO. However, in this system, all the states, i.e., MO, SC, NFL, and FL, are fairly sensitive to pressure at around the critical pressure of 11 GPa; the QC behavior emerges quite sharply. The quantity $\sqrt{A}$ in the figure, which is proportional to the enhanced effective electron mass m^*, decreases substantially with pressure. The magnetism and bulk SC seem to coexist only in the critical region. At higher temperatures over 100 K the resistivity shows the Kondo effect (KE); see the inset of Fig. 1(b).

The present results are compared with the pressure effects on the paramagnetic superconductor $LaNiC_2$ [17]. Those results indicated that its SC could be related to a QC feature with strong electronic correlations, most likely a charge density wave (CDW). The emergence of SC in magnetic $CeNiC_2$ can be connected with magnetic fluctuations originated from its MO.

As shown before, SC appears at a rather high temperature of 3.5 K. According to the SF theory, the T_c of high-T_c cuprates and heavy-fermion superconductors can be correlated with the frequency spread of their antiferromagnetic fluctuations T_0. Here, T_0 is given with the coefficient of the electronic specific heat γ as $\approx 12\,500/\gamma$ [18]. For $CeNiC_2$ we now have no information about γ under the critical pressure; however, with a relation $\gamma \approx R \ln 2/T_K$ for the doublet ground state (R is the molar gas constant and T_K is the Kondo temperature), γ is roughly evaluated to be 600 $mJ/mol\,K^2$ because its T_K is reported as ~10 K [19]. This γ seems to be relevant since γ at ambient pressure is about 300 $mJ/mol\,K^2$ [5] and in the SF model γ will be enhanced at the critical region. Supposing $\gamma \sim 600$ $mJ/mol\,K^2$, we have $T_c \sim 0.7$ K from the figure of Ref. [18]. If these estimations are appropriate, T_c observed at 3.5 K is much higher than that estimated with γ in the SF model. Thus, to explain such a strong enhancement of T_c in the experiment, other factors would be necessary. Some *exotic* mechanism with a higher-energy scale, such as a valence-fluctuation (VF) model [20], is a candidate to explain the high T_c.

To other NCS Ce-based superconductors, T_c's were reported as ~1 K and γ as ~100 $mJ/molK^2$ [3,12–14]. The relationship between T_c and T_0 indicated above gives T_c of ~5 K [18]; the systematically and fairly low T_c's observed in the experiments might be due to the spin-triplet nature of their SC or some other features not included in SF

The magnetic field effects on the resistivity are indicated in Fig. 4. The maximum field was 5 T. The pressure applied

was 11.4 GPa. Only a clamp-type pressure cell could be used for this experiment; therefore the tuning of pressure at around 11 GPa was difficult. SC under this pressure shows a transition with a width of about 1 K, as observed previously. The results show that this SC is quite robust in magnetic fields. The slope of $\mu_0 H_{c2}$ near $H = 0$, $d(\mu_0 H_{c2})/dT \equiv \mu_0 H'_{c2} \sim -7.1$ T/K for the onset resistivity, whose $T_c(H = 0)$ of 3.5 K is the same as that under the critical pressure of 11 GPa. The slope of $\mu_0 H_{c2}$ for the zero resistivity, $T_c \sim 2.5$ K, is similar to that for the onset data. From the empirical parabolic relation, $H_{c2}(T)/H_{c2}(0) = 1 - t^2$ ($t = T/T_c$), $\mu_0 H_{c2}$ at $T = 0$ is roughly estimated to be 20 T. This field is much higher than the Pauli paramagnetic limiting field $\mu_0 H_P^{BCS}$ of 6.5 T evaluated from $\Delta/(\sqrt{2}\mu_B) \approx 1.86 T_c$; here, Δ is the superconducting energy gap. This high $\mu_0 H_{c2}$ indicates that SC of the system is likely a spin triplet. Such an unusual triplet state has been established in subsequent studies for all other NCS Ce-based SC with quite high $\mu_0 H_{c2}$'s. The spin triplet proposed here also corresponds with its NCS structure of the system. This spin-triplet state, however, as well as the coexistence with the spin-singlet state, should be examined further.

From the formula $\mu_0 H_{c2} = \Phi/(2\pi\xi^2)$, where Φ is the flux quantum, the Ginzburg-Landau (GL) coherence length ξ is obtained to be 4.2×10^{-9} m experimentally. This ξ is comparable with the Pippard coherence length ξ_0 (~the size of the interacting pairs, given by the conventional BCS theory as $\xi_0 = 0.18\hbar v_F/k_B T_c$ with the Fermi velocity v_F), i.e., $\xi \sim \xi_0$ at $T = 0$ [21]. Physically, when the distance between vortices becomes equal to that between interacting electrons, SC would collapse. When we assume a spherical Fermi surface with $\gamma \sim 600$ mJ/mol K^2 in the SF model before, ξ_0 is evaluated to be $\sim 0.7 \times 10^{-9}$ m, which is rather shorter than the GL coherence length ξ obtained above; such a discrepancy suggests again that the present SC is not explained well with the SF model. Supposing that $\gamma \sim 100$ mJ/mol K^2, which is considerably smaller than that assumed in SF, ξ_0 will be rightly $\sim 4 \times 10^{-9}$ m of ξ above. The decrease in γ near the critical pressure such as this, caused by the valence changes there, is a characteristic of the VF model referred to previously. Moreover, the results observed, i.e., the higher T_c, the fairly sharp QC compared with those in SF, and the enhanced T-linear dependence of ρ (which should be dimension-independent), are also reasonably explained by VF [20]. Noted that the relationship between T_c and T_0 based on SF shown before would not be simply applicable to VF.

The v_F estimated from ξ above, with the residual resistivity $\rho_0 \sim 20\ \mu\Omega$ cm, gives the mean free path l ($= v_F\tau$; here, τ is a relaxation time $\propto m^*/\rho_0$) $\sim 1 \times 10^{-8}$ m. This value is larger than ξ, indicating that the system is in the clean limit. In this case the orbital limiting field is calculated from $\mu_0 H_{orb}^{BCS} = 0.727(-\mu_0 H'_{c2}) T_c$ [22]. Using the slope of $\mu_0 H_{c2}$ before, $\mu_0 H_{orb}^{BCS}$ at $T = 0$ is obtained to be 18 T, consistent with that estimated roughly before. The lines in Fig. 4 show fits to the Werthamer-Helfand-Hohenberg (WHH) theory. Note that the sample used is a polycrystal; when the SC has strong anisotropy, $\mu_0 H_{c2}$ of the system could be higher than 18 T.

As displayed in Fig. 4, $\mu_0 H_{c2}$ for $LaNiC_2$ observed in our resistivity and magnetization measurements is as small as about 0.3 T, which is very low compared with the calculated $\mu_0 H_P^{BCS}$ of 5.5 T for $T_c \sim 3$ K. On this SC, the nonunitary triplet state was proposed from a muon spin relaxation (μSR) experiment and group theoretical discussions [23,24]. The very low $\mu_0 H_{c2}$ of $LaNiC_2$, however, with other results referred to in Ref. [7], may suggest that its SC could be a spin singlet. The "nonunitarity" might be expected for the spin-triplet state implied for this $CeNiC_2$, since the discussion on $LaNiC_2$ with the point group C_{2v} mentioned above would be equally applied to this system. Noted that $CeNiC_2$ has the F phase exhibiting a spontaneous magnetization [9].

With the coherence length ξ_0 and $\gamma \sim 100$ mJ/mol K^2, the number $k_F\xi_0$ is calculated to be ~40 (k_F is the Fermi momentum given by $m^* v_F/\hbar$, and $1/k_F$ is the average distance between electrons). This number is rather small. The ratio Δ/E_F (E_F is the Fermi energy) is ~0.02, and is fairly large. Compare them with those estimated for $CePt_3Si$: $k_F\xi_0 \sim 90$ and $\Delta/E_F \sim 0.005$. The characteristic values indicated above further imply that this SC is exotic, reflecting the short coherence length ξ_0 and the high T_c, thus the strong electron couplings.

To conclude, high-pressure experiments on magnetic NCS $CeNiC_2$ have shown a unique SC. Its T_c is quite high, 3.5 K under 11 GPa. The QC behavior observed is rather sharp against pressure. The specific features observed could be understood by a model such as VF with a high-energy process. The $\mu_0 H_{c2}$ evaluated for $T = 0$ is as high as 18 T, indicating that this SC has a spin-triplet nature in connection with its peculiar *Amm*2 NCS.

S.K. acknowledges valuable discussions with J. Quintanilla and K. Miyake.

[1] J. Bardeen, L. N. Cooper, and J. R. Schrieffer, Phys. Rev. **106**, 162 (1957); **108**, 1175 (1957).
[2] P. W. Anderson, Phys. Rev. B **30**, 4000 (1984).
[3] E. Bauer, G. Hilscher, H. Michor, Ch. Paul, E. W. Scheidt, A. Gribanov, Yu. Seropegin, H. Noël, M. Sigrist, and P. Rogl, Phys. Rev. Lett. **92**, 027003 (2004).
[4] P. A. Frigeri, D. F. Agterberg, A. Koga, and M. Sigrist, Phys. Rev. Lett. **92**, 097001 (2004).
[5] S. Katano, K. Shibata, K. Nakashima, H. Yoshimura, and Y. Matsubara, J. Phys. Soc. Jpn. **86**, 104704 (2017).
[6] Z. F. Weng, J. L. Zhang, M. Smidman, T. Shang, J. Quintanilla, J. F. Annett, M. Nicklas, G. M. Pang, L. Jiao, W. B. Jiang, Y. Chen, F. Steglich, and H. Q. Yuan, Phys. Rev. Lett. **117**, 027001 (2016).
[7] S. Katano, K. Shibata, K. Nakashima, and Y. Matsubara, Phys. Rev. B **95**, 144502 (2017).
[8] K. Motoya, K. Nakaguchi, N. Kayama, K. Inari, J. Akimitsu, K. Izawa, and T. Fujita, J. Phys. Soc. Jpn. **66**, 1124 (1997).
[9] V. K. Pecharsky, L. L. Miller, and K. A. Gschneidner, Jr., Phys. Rev. B. **58**, 497 (1998).
[10] J. Gouchi *et al.* (unpublished).
[11] J.-G. Cheng, K. Matsubayashi, S. Nagasaki, A. Hisada, T. Hirayama, M. Hedo, H. Kagi, and Y. Uwatoko, Rev. Sci. Instrum. **85**, 093907 (2014).

[12] N. Kimura, K. Ito, K. Saitoh, Y. Umeda, H. Aoki, and T. Terashima, Phys. Rev. Lett. **95**, 247004 (2005).
[13] I. Sugitani, Y. Okuda, H. Shishido, T. Yamada, A. Thamizhavel, E. Yamamoto, T. D. Matsuda, Y. Haga, T. Takeuchi, R. Settai, and Y. Ōnuki, J. Phys. Soc. Jpn. **75**, 043703 (2006).
[14] T. Kawai, H. Muranaka, M.-A. Measson, T. Shimoda, Y. Doi, T. D. Matsuda, Y. Haga, G. Knebel, G. Lapertot, D. Aoki, J. Flouquet, T. Takeuchi, R. Settai, and Y. Ōnuki, J. Phys. Soc. Jpn. **77**, 064716 (2008).
[15] V. A. Sidorov, M. Nicklas, P. G. Pagliuso, J. L. Sarrao, Y. Bang, A. V. Balatsky, and J. D. Thompson, Phys. Rev. Lett. **89**, 157004 (2002).
[16] T. Moriya and K. Ueda, Rep. Prog. Phys. **66**, 1299 (2003).
[17] S. Katano, H. Nakagawa, K. Matsubayashi, Y. Uwatoko, H. Soeda, T. Tomita, and H. Takahashi, Phys. Rev. B **90**, 220508(R) (2014).
[18] S. Nakamura, T. Moriya, and K. Ueda, J. Phys. Soc. Jpn. **65**, 4026 (1996).
[19] A. Bhattacharyya, D. T. Adroja, A. M. Strydom, A. D. Hillier, J. W. Taylor, A. Thamizhavel, S. K. Dhar, W. A. Kockelmann, and B. D. Rainford, Phys. Rev. B **90**, 054405 (2014).
[20] A. T. Holmes, D. Jaccard, and K. Miyake, Phys. Rev. B. **69**, 024508 (2004).
[21] M. Tinkham, *Introduction to Superconductivity* (McGraw-Hill, New York, 1975), p. 10.
[22] E. Helfand and N. R. Werthamer, Phys. Rev. **147**, 288 (1966).
[23] A. D. Hillier, J. Quintanilla, and R. Cywinski, Phys. Rev. Lett. **102**, 117007 (2009).
[24] J. Quintanilla, A. D. Hillier, J. F. Annett, and R. Cywinski, Phys. Rev. B **82**, 174511 (2010).

Correction: The third paragraph from last contained a source citation error and has been fixed.